Modeling analysis of molecular chiral effect detected by Maxwell-displacement-current measurements

Wei Zhao, Chen-Xu Wu, Mitsumasa Iwamoto, and Ou-Yang Zhong-can

Citation: J. Chem. Phys. **110**, 12131 (1999); doi: 10.1063/1.479150

View online: http://dx.doi.org/10.1063/1.479150

View Table of Contents: http://jcp.aip.org/resource/1/JCPSA6/v110/i24

Published by the AIP Publishing LLC.

Modeling analysis of molecular chiral effect detected by Maxwell-displacement-current measurements

Wei Zhao, Chen-Xu Wu, and Mitsumasa Iwamoto[a)]
Department of Physical Electronics, Tokyo Institute of Technology, 2-12-1 O-okayama, Meguro-ku, Tokyo 152-8552, Japan

Ou-Yang Zhong-can
Institute of Theoretical Physics, Academia Sinica, P.O. Box 2735, Beijing 100080, China

(Received 12 January 1999; accepted 1 April 1999)

Based on Maxwell displacement current (MDC) and surface pressure measurements by monolayer compression, the physicochemical properties of chiral and racemic phospholipid [α-phosphatidylcholine dipalmitoyl (DPPC)] monolayers at the air–water interface were investigated. It was found that at a temperature of 20 °C, the chiral and racemic phospholipid monolayers exhibited similar pressure-area isotherms with a pressure plateau between 65 and 85 Å^2, usually attributed to the two-dimensional (2D) phase transition from expanded monolayer to condensed one. Nevertheless, with MDC measurement some critical peaks in the 2D pressure plateau region with different amplitude and sign were detected related to the chirality of the phospholipid samples. This result clearly demonstrates that microscopic chirality affects the electrical properties of monolayers. To investigate the chiral effect theoretically, a twist-conformation molecular model was raised by a modification of the simple rodlike model and biaxial rodlike model, which were developed in our previous work. The analysis based on this modified model reveals that the monolayer properties, especially the MDC behavior by compression, are profoundly influenced by the chirality of molecules. © *1999 American Institute of Physics.* [S0021-9606(99)70724-5]

I. INTRODUCTION

Organic monolayers at the air–water interfaces composed of amphiphiles are quasi-2D systems with much interest owing to their abundant phenomena including their phase diversity, their close similarity to biological membrane, and the possibility of using them to explore the physicochemical properties of membrane structures.[1,2] The possible application in molecular electronics, biosensors, and so on is a critical promotion of the study of monolayers and makes it a rather urgent study subject. The investigation about monolayers can be traced back to Langmuir, who constructed the well-known apparatus (Langmuir trough) to measure the 2D pressure of the air–water interfacial monolayer,[3] and Blodgett, who developed the technique to pile up monolayers into tens and even hundreds of layers, which in some aspects has great convenience for researching monolayers.[4] After that much progress has been made, both in the recognition of the physicochemical properties of monolayers and the measurement implements, techniques, and methodologies. For the former aspect, many phases of monolayers have been found; the corresponding phase transitions and related behaviors have been investigated extensively, both experimentally and theoretically.[1,2] For the latter, several methodologies, such as x-ray and neutron reflectometry, second harmonic generation method, fluorescence microscopy, and surface potential technique, which are effective to study monolayers at the air–water interface or transferred to the air–solid interface, have been established. Nevertheless, most of them are more appropriate for the investigation of the static than for the dynamic properties of monolayers. On the other hand, some of these methods, because of inherence, have to perform a transfer from air–liquid interface to air–solid interface and even a Langmuir–Blodgett technique to pile up the monolayers into multilayers. Although these transfer and piling are with rather importance and are helpful to the study of monolayer properties, the investigations based on these techniques are worth being suspected owing to the possibility of the destruction of the monolayers. The surface pressure measurement method, which is appropriate for studying the organization properties of monolayers directly at the air–water interface, and has performed a very important role in the history of monolayer investigation, under the present point of view, may not be enough. So, it is urgent to construct a method which is applicable to the investigation of organization properties of monolayers and the direct measurement at the air–water interface. In recent years we have been exploring the MDC measurement technique which is suitable for the aforementioned requests.[5] With this technique we have performed many studies about the monolayers at the air–water interfaces. We found the MDC technique rather helpful for the investigation of monolayer properties.

Another essential point in the present work is chirality. Chirality is a concept with rather importance in physics,

a)Author to whom correspondence should be addressed. Electronic mail: iwamoto@pe.titech.ac.jp

chemistry, biology, and geology.[6,7] An astonishing phenomenon is the biomolecular homochirality of all lives on the earth, which means that all amino acids, which are the elementary unit of proteins in organisms, are levorotatory.[8] This homochirality has been giving rise to extensive consequences in pharmacology, medicine, physiology, and even ecology. In geology, many minerals have two chiral states, such as quartz, but more frequent situation is a kind of mineral with molecular chirality but macroscopic achirality, i.e., the racemic state.[6] Because of these, chirality has long been an important concept in chemistry and physics. Some subjects, such as chiral phase separation (CPS), chiral symmetry breaking (CSB), are with more and more significance. Historically, the first time when chirality was related to chemistry may be the manual resolution of the crystals of sodium ammonium tartarate tetrahydrate by Pasteur.[9] The development of organic chemistry and stereochemistry more emphasized the significance of chirality. The macroscopic effect and microscopic origin of the chirality are topics of chemical physics. In the former aspect, a great amount of work has been done about cholesteric liquid crystals (ChLC), chiral biomembranes, and so on. Whereas in the latter aspect, although some molecular models have been established, our knowledge may be far from enough. Reference 10 is a work about this topic. Although the thought is beautiful and the result is undoubtedly important, further investigation and the extension of this model may not be easy.

The combination of the above two points leads to the concept of chiral monolayers. Air–water interfacial monolayers are easily accessible and show several phases during compression. Therefore, the study of the effects of molecular chirality on the monolayer phase behavior may have important meaning to reveal the biological and chemical consequences of the molecular handedness. This is the starting point of our present work, in which the piezoelectric behaviors and the 2D pressure-area ($\pi-A$) isotherms of phosphatidylcholine dipalmitiyl (DPPC) monolayers composed of dextro-(D-), levo-(L-) rotatory molecules as well as the racemic molecular compound (DL-DPPC) have been measured. DPPC is one of phospholipids (PCL) which are among the main amphiphiles of biomembranes. Each DPPC molecule contains one phosphatidylcholine (polar hydrophilic) head group and two long alkyl chains, each with a carbonyl (hydrophobic) group connected by a glyceryl. The middle carbon atom of the glyceryl is a chiral center owing to the four groups connected to it being different with every each other. Figure 1 shows the schematic of the D-DPPC molecule (for L-DPPC it is just the mirror image of D-DPPC). Our experiment shows that for DPPC monolayers of the two pure enantiomers, and the racemic molecular compound (DL-DPPC), although the $\pi-A$ isotherms are similar to each other, the MDC behaviors of them are critically different depending on the molecular chirality.

From the theoretical point of view, in a series of foregoing works we established a rodlike molecular model with uniaxial or biaxial symmetry to microscopically describe the piezoelectric properties of monolayers[11] and compression-induced orientational transition of monolayer.[12] Yet the previous model which is achiral is not enough for the present problem in which the molecular handedness is involved. In our recent paper,[13] we modified the achiral rodlike model into chiral twist one briefly. Here we discuss the result of this revised model further and in greater detail. It is revealed for the first time through a lengthy calculation and computation that both the orientational order parameter and the MDC current are related to the chirality of the component molecules. Although this model is rather conceptive, these results strongly indicate that macroscopic handedness is profoundly influenced by microscopic, especially molecular, chirality.

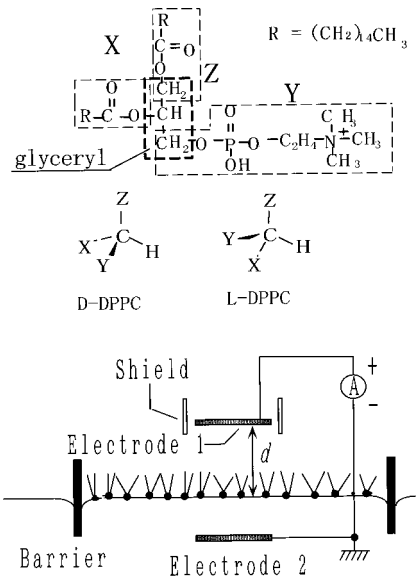

FIG. 1. Schematic diagram for DPPC molecule (upper) and experimental setup (below).

II. EXPERIMENT

A. Experimental setup

Besides the detailed molecular form of D-DPPC, Fig. 1 shows the schematic of our experimental setup used in the present investigation.[13,14] The principal part is a Langmuir trough in rectangular shape with dimensions 15 cm×73 cm. A Wilhelmy-type film balance system is connected to it to measure the 2D pressure. Two electrodes 1 and 2 parallel to the water surface are connected with each other through a sensitive ammeter, with electrode 1 suspended in the air above the water surface and electrode 2 immersed in the water subphase. The effective working area of electrode 1 is 45.6 cm^2 and the spacing between electrode 1 and water surface (d) is manually adjusted to 1.15 mm. The water subphase (pH 6) is kept at a constant temperature of 20 $\pm 0.2\,^{\circ}C$. The monolayers of D-, L-, and DL-DPPC are formed on the water surface by spreading their dilute chloroform solutions onto the water surface of the Langmuir trough using a microcyringe. The three samples used in the experiment were purchased from SIGMA, and they were used as received without further purification. The monolayers of DPPC formed on the water surface were compressed with two floating barriers at a constant barrier velocity of 40 mm/min, i.e., the monolayers were compressed at a constant

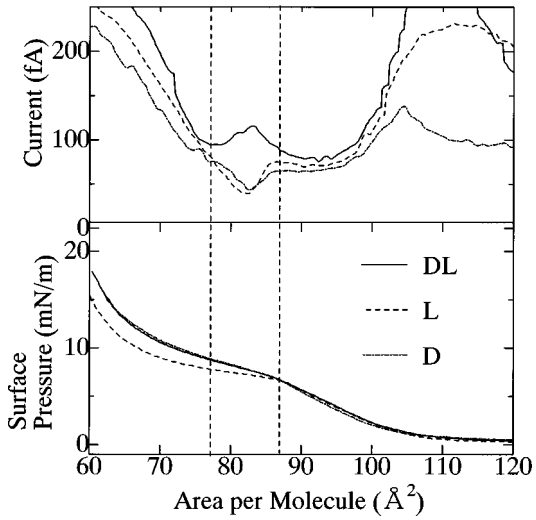

FIG. 2. Maxwell displacement currents (above) measured in DPPC monolayers composed of pure L-DPPC, D-DPPC, and DL-DPPC, respectively.

speed of 0.081 Å^2/s. The MDC-molecular area (MDC-A) curves and $\pi-A$ isotherms were simultaneously measured during the monolayer compression.

B. Results

Figure 2 shows the typical experimental results of the measurement for the three samples: Pure L-DPPC, D-DPPC, and DL-DPPC monolayers, respectively. As shown in Fig. 2, the $\pi-A$ isotherms of the three samples are almost the same function of molecular area A containing nearly the same pressure plateau in the range of 65–85 Å^2 of molecular area. The plateau was usually referred to 2D phase transition region from the expanded monolayers to condensed one. In Ref. 15, with the help of the x-ray diffraction, the 2D positional transition was also argued to associate with the molecular conformation change from bent chain state to straight chain state. In our recent work,[13,14] the plateau region is interpreted to involve the phase transition of molecular orientation from isotropic to polar orientation. From the present $\pi-A$ measurement, it seems that the mentioned phase transitions are obviously independent of the chirality of the molecules composed in the monolayers. However, the result of MDC measurement shown in Fig. 2 (upper) reveals that although the main shapes of the MDC viewed as a function of the molecular area A are roughly similar for the four samples, there exist some essential differences between them: The most striking characteristic is the generation of MDC peak that appears in the beginning of the pressure plateau, $A=85$ Å^2, with different amplitude and sign for the chiral and racemic examples. The MDC curve of pure D-DPPC is similar to that of L-DPPC, with a downward peak at the beginning of the pressure plateau, whereas the racemic compound DL-DPPC has an upward peak in its MDC at the same molecular area. Although the amplitude may look minor as contrasted with the large MDC strength in $A>90$ Å^2 region, the very good reappearance of these anomalous peaks strongly emphasized their significance. Contrarily, the MDC profiles in $A>90$ Å^2 region are somewhat unstable and the reappearance is not so good. In Fig. 2 the MDC of L- and D-DPPC appear different in this region, although the symmetry of chirality determines that both enantiomers be identical. Here we point out that the difference is only an appearance of this instability. The cause of the instability is still not clear and now in further experimental investigation. From the viewpoint of molecular level, the three examples of the DPPC monolayers differ from each other only in their chirality: DL-DPPC molecule is racemic, whereas L-DPPC and D-DPPC both are chiral with different optical activity. Therefore, the mentioned anomalous MDC peak should reveal some molecular conformation properties relating to the molecular chirality. In other words, this anomalous MDC generation may be of significant help to understand the chiral discrimination from molecular conformation level. Here we present a theory to describe the chirality dependence of the MDC peak of a monolayer, and discuss the anomalous MDC generation.

III. ANALYSIS

A. Development of the model

The uniaxial and biaxial rodlike molecular model both are used in our previous work.[11] The molecule of uniaxial model is represented by a rod with C_∞ symmetry and a dipole coincided with the long axis of the rod. Yet in the biaxial model the molecular dipole is attached to the rod with a finite cross angle θ_D. So the biaxial molecule is with C_2 symmetry. The previous models were used to analyze the piezoelectric properties of usual monolayers, the normal-tilted orientational phase transition and several other topics.[11,12] However, they are not enough for analysis of the present problem: The MDC behavior of chiral monolayers. It is easy to see that the previous models are both nonchiral because of the existence of the mirror plane symmetry: For the uniaxial model, any plane including the molecular long axis is its symmetry mirror; for the biaxial model, the plane including the molecular long axis and the dipole direction is its symmetry mirror too. Our experiment irrefutably shows that the chirality of the consistent molecules affects the MDC behavior and the dielectric properties of monolayers, at least in the range involving the anomalous MDC generation, as shown in Fig. 2. Therefore, we may expect that the chiral symmetry of monolayers can be described by the modification of the previous models. We have advanced a new model with no mirror plane symmetry and simply performed its direct results in our recent work.[13] Now we devote to further demonstrating the consequences of this model.

The basic geometry used in the present theory is shown in Fig. 3. It remains to be one dipole model. Nevertheless, the dipole **P** is not located on the molecular long axis but on a cylindrical surface. The cylinder may only be a virtual existence just for the easy understanding of the present model, but for some cases it can also have some factual counterpart, for example, the molecule 12HOA described in Ref. 15. In the present model the cylinder can be regarded as the *trans*-alkane chain of 12HOA and the dipole expresses that of the hydroxyl group.

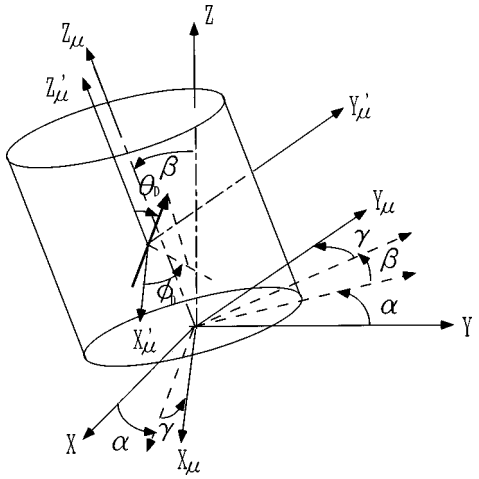

FIG. 3. Sketch of rodlike molecular model for PCL monolayers at the air–water interface. The cylinder represents the molecular long axis and the side dipole flanking the cylinder with polar angle θ_D and twist angle ϕ_D. The latter serves to describe the chirality of the molecules, $\phi_D=0$ and π for racemic, otherwise for chiral.

Described in the molecular frame, the dipole position is

$$\mathbf{r}_0=(x_\mu,y_\mu,z_\mu)=(a,0,h), \tag{1}$$

where z_μ is along the molecular long axis. Besides an angle θ_D $(0\leqslant\theta_D\leqslant\pi)$ away from $\mathbf{z}_\mu$, it is assumed that dipole is not in the plane of $y_\mu=0$, but with a tilted angle ϕ_D to it $(0\leqslant\phi\leqslant2\pi)$, i.e., in the molecular frame

$$\mathbf{P}/P=(\sin\theta_D\cos\phi_D,\sin\theta_D\sin\phi_D,\cos\theta_D). \tag{2}$$

It is easy to check that $\phi_D\neq0$ represents the chirality and $\phi_D=0$ and π mean nonchiral states with biaxiality ordering.[10]

Other geometry of the monolayer composed of the dipolar molecules is the same as that in Ref. 11, as illustrated in Fig. 3: The average orientation of the molecular long axis is upright to the water surface and referred to the z direction of the laboratory frame. (Although several phases including tilt direction state are possible,[2] in this work we will only consider the simplest and the most common one: The uniaxial phase with the average dipole orientation normal to the monolayer plane. This is similar to the S_A^* phase in liquid crystals.[16] Here we also name it as S_A^* phase.) It is then obvious that the molecular orientation is confined in the range of $0\leqslant\beta\leqslant\theta_A=\arcsin\sqrt{A/A_0}$ (see Fig. 3) due to the effect of hardcore intermolecular repulsive force working among molecules, where β is the angle between $\mathbf{z}$ and the molecular long axis, $A_0=\pi l^2$ is the critical molecular area, l is the partial length of the molecules along their long axis above the water surface, and A is the mean molecular area. The angle γ in Fig. 3 is the azimuth of the molecular long axis.

We express the angle of the dipole direction from $\mathbf{z}$ as θ_L and the angle between $\mathbf{z}$ and the position vector of the dipole $\mathbf{r}_0$ as θ', respectively. To describe the apparent relations of both θ_L and θ' with the geometry given in Fig. 3, we introduce the relationship between the molecular frame $\mathbf{r}_\mu=(x_\mu,y_\mu,z_\mu)$ and the laboratory one $\mathbf{r}=(x,y,z)$ with Euler angles (α,β,γ) defined as the convention in Ref. 17. Then we have, in the molecular frame

$$\mathbf{z}/z=(\sin\beta\sin\gamma,\sin\beta\cos\gamma,\cos\beta). \tag{3}$$

From Eqs. (1)–(3), we obtain

$$\cos\theta_L=(\mathbf{z}/z)\cdot(\mathbf{P}/P)=\sin\theta_D\sin\beta\sin(\gamma+\phi_D)+\cos\theta_D\cos\beta,$$

$$r_0\cos\theta'=\mathbf{r}_0\cdot(\mathbf{z}/z)=a\sin\beta\sin\gamma+h\cos\beta. \tag{4}$$

We reasonably assume that the angular position of the molecules obeys Boltzmann's law, and write the molecular distribution function as

$$f(\beta,\gamma)=\frac{\exp[-W(\beta,\gamma)/kT]}{Z}, \tag{5}$$

where W is the interaction working on a monolayer molecule, and Z is the single-particle partition function given by

$$Z=\int_0^{2\pi}d\gamma\int_0^{\theta_A}\exp[-W(\beta,\gamma)/kT]\sin\beta d\beta. \tag{6}$$

Here k is the Boltzmann constant and T is the temperature.

We have defined the orientational order parameter for the previous uniaxial and biaxial model.[11] Concerning the electrical properties of the monolayer, similarly we define the polar orientational order parameter as

$$S=\langle\cos\theta_L\rangle=\frac{1}{Z}\int_0^{2\pi}d\gamma\int_0^{\theta_A}\cos\theta_L\exp[-W/kT]\sin\beta d\beta. \tag{7}$$

It means the average dipole direction of the molecules. The MDC behavior of the monolayer is intimately related to it.

B. Interactions working on monolayer molecules

Besides the hardcore repulsive force, there are also two kinds of interactions working on the molecules. One is the attractive Coulomb force working with the image of the molecular dipole in the bulk water, given by Ref. 18

$$W_s(\beta,\gamma)=-P^2\left(\frac{\epsilon_w-\epsilon_m}{\epsilon_w+\epsilon_m}\right)\frac{1+\cos^2\theta_L}{32\pi\epsilon_0(r_0\cos\theta')^3}, \tag{8}$$

where ϵ_m and ϵ_w are the relative dielectric constants of monolayer and the water, respectively, ϵ_0 is the permittivity of free space, and $d=r_0\cos\theta'$ is the distance of the dipole above the water surface with $r_0=|\mathbf{r}_0|=\sqrt{a^2+h^2}$.

The other interaction is that working on the considered molecule by all the other molecules of the monolayer. The origin of this intermolecular interaction is the dipole–dipole electrostatic Coulomb force (Fig. 4) with the form[18]

$$W_{1,2}=-\frac{P^2[2\cos\theta_1\cos\theta_2-\sin\theta_1\sin\theta_2\cos\phi]}{4\pi\epsilon_0 r^3}, \tag{9}$$

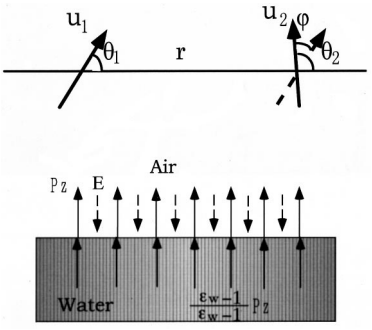

FIG. 4. Schematic of the intermolecular dipole–dipole interaction (upper) and mean-field approach (lower).

where r is the distance between them along their positional connecting line **l**; θ_1 and θ_2 are their tilted angles with respect to **l**, respectively; ϕ is the difference between the azimuthal angles of $\mathbf{P}_1$ and $\mathbf{P}_2$.

The total interaction working on a consistent molecule is the sum of W_s and W_e

$$W = W_s + W_e, \tag{10}$$

where $W_e = \Sigma_i' W_{1,i}$ with $i=1$ representing the considered molecule at the origin. The sum Σ_i' includes all the real and image dipoles of the monolayer molecules except the one at the origin.

C. Mean electrical field of S_A^* monolayer

A complete and detailed consideration of the intermolecular dipole–dipole interaction would lead to rather complication, so some simplification may be necessary. In the present work, we use a mean-field approach to deal with these intermolecular interactions (see Fig. 4).

As mentioned above, any constituent molecule has a dipole

$$\mathbf{P} = \mathbf{P}_\parallel + \mathbf{P}_z, \tag{11}$$

where $\mathbf{P}_\parallel$ and $\mathbf{P}_z$ are components parallel and normal to the monolayer plane, respectively. Each molecular dipole **P** is accompanied by an image dipole

$$\mathbf{P}_i = \frac{\epsilon_w - 1}{\epsilon_w + 1}(-\mathbf{P}_\parallel + \mathbf{P}_z). \tag{12}$$

As was discussed in Ref. 19, we omit the effect of the dipole-image positional spacing. Under the point of view of other molecules, the considered one induces the electrical field as if it had a dipole

$$\mathbf{P} + \mathbf{P}_i = \frac{2}{\epsilon_w + 1}\mathbf{P}_\parallel + \frac{2\epsilon_w}{\epsilon_w + 1}\mathbf{P}_z. \tag{13}$$

Noting that $\epsilon_w = 81 \gg 1$, the effect of the parallel component is far less than that of the normal component. On the other hand, for S_A^* phase monolayer, the effect of the parallel component may be almost counteracted with each other owing to the isotropic distribution of the parallel component. With these two reasons we omit the parallel component of the total molecular dipole and only consider the normal one. Consequently, all the molecules except the original one produce a total field at the origin

$$\sum_i{}' \mathbf{E}_i = -\frac{2\epsilon_w}{\epsilon_w + 1}\frac{P}{4\pi\epsilon_0}\sum_i{}' \frac{(\cos\theta_L)_i}{r_i^3}\frac{\mathbf{z}}{z}. \tag{14}$$

The effective field working on the original dipole is the thermodynamical average of $\Sigma_i' \mathbf{E}_i$

$$E = \left|\left\langle \sum_i{}' \mathbf{E}_i \right\rangle\right| = -gPa^{-3/2}S, \tag{15}$$

where S is the order parameter defined before, $a = A/A_0$, and g is a parameter defined for convenience,

$$g = \frac{2\epsilon_w}{\epsilon_w + 1}\frac{1}{4\pi\epsilon_0}a^{3/2}\sum_i{}' \frac{1}{r_i^3}.$$

It is a constant in the compression process if there is no positional order phase transition. Thus the intermolecular action W_e in Eq. (10) is simplified to a mean field potential

$$W_e(\beta,\gamma) = -\mathbf{P}\cdot\mathbf{E} = gP^2a^{-3/2}S\cos\theta_L. \tag{16}$$

The question is obviously a self-consistent one since the orientational order parameter or the molecular distribution is involved in the energy of a molecule.

IV. CALCULATION OF THE ORIENTATIONAL ORDER PARAMETERS

A simultaneous consideration of energy W_e and W_s would lead the question to a very difficult situation because of the complication of the total energy W. So by following Ref. 19, we only consider two limit cases at the present work: (1) for $|W_s| \gg |W_e|$, and (2) for $|W_s| \ll |W_e|$. The former case occurs as the molecular area A is close to the critical area A_0, whereas the latter one takes place only if the area per molecule is much smaller than the critical area A_0.

A. In the case of $|W_s| \gg |W_e|$

In this case, by omitting W_e and using the approximation in a manner as carried out by Onsager,[20] the Boltzmann factor becomes

$$\exp[-W(\beta,\gamma)/kT] = 1 - W(\beta,\gamma)/kT. \tag{17}$$

The single-particle partition function defined in Eq. (6) becomes

$$Z = 2\pi[1-\cos\theta_A] + P^2\left(\frac{\epsilon_w - \epsilon_m}{\epsilon_w + \epsilon_m}\right)\frac{1}{32\pi\epsilon_0 kT} \times \int_0^{\theta_A}\int_0^{2\pi}\Omega\sin\beta d\beta d\gamma, \tag{18}$$

where

$$\Omega=\frac{1+\cos^2\theta_L}{(r_0\cos\theta')^3}$$

$$=[1+\cos^2\theta_D\cos^2\beta+\sin^2\theta_D\sin^2\theta\sin^2(\gamma+\phi_D)+2\sin\theta_D\cos\theta_D\sin\beta\cos\beta\sin(\gamma+\phi_D)]/(a\sin\beta\sin\gamma+h\cos\beta)^3.$$

After a lengthy integration as shown by Eqs. (A1)–(A4) in Appendix A, we get the single-particle partition function

$$Z=Z(A,\theta_D,\phi_D)=2\pi[1-\cos\theta_A]+\pi\eta\Big\{(1+\cos^2\phi_D\sin^2\theta_D)[\tan^2\psi\sin^{-3}\alpha-(1+\tan^2\psi)\sin^{-1}\alpha]$$
$$+(\cos^2\theta_D-\cos^2\phi_D\sin^2\theta_D)\Big[(3\cos^2\psi-2)(\sin^{-1}\psi-\sin^{-1}\alpha)-\sin^2\psi(\sin^{-3}\psi-\sin^{-3}\alpha)$$
$$+(2-3\cos^2\psi)\ln\frac{1+\sin\psi}{(1+\sin\alpha)\cos\theta_A}\Big]+\sin^2\theta_D(2\cos^2\phi_D-1)\Big[\tan^2\psi(\sin^{-1}\psi-\sin^{-1}\alpha)$$
$$+\ln\frac{1+\sin\psi}{(1+\sin\alpha)\cos\theta_A}\Big]-\sin 2\theta_D\cos\phi_D\sin\psi\cos\psi\Big[3(\sin^{-1}\psi-\sin^{-1}\alpha)$$
$$-\tan^2\psi(\sin^{-3}\psi-\sin^{-3}\alpha)-3\ln\frac{1+\sin\psi}{(1+\sin\alpha)\cos\theta_A}\Big]\Big\}, \tag{19}$$

where θ_A was defined above, $\tan\psi=h/a$, and $\cos\alpha=\cos\psi/\cos\theta_A$. The dimensionless parameter $\eta=P^2[(\epsilon_w-\epsilon_m)/(\epsilon_w+\epsilon_m)]/32\pi\epsilon_0 r_0^3 kT$ describes the relative strength of the dipole-medium interaction energy with respect to the thermal energy kT.

To investigate the dielectric properties of monolayers and the MDC behavior by compression, the average dipole moment $\langle P_z\rangle=PS$ is necessary to be calculated, where S is the orientational order parameter

$$S=\frac{1}{Z}\int_0^{2\pi}d\gamma\int_0^{\theta_A}\cos\theta_L\left(1-\frac{W}{kT}\right)\sin\beta d\beta. \tag{20}$$

In the actual calculation, for the sake of simplicity, we take an approximation of

$$-\cos\theta_L\frac{W}{kT}=\frac{\eta r_0^3(\cos\theta_L+\cos^3\theta_L)}{(a\sin\beta\sin\gamma+h\cos\beta)^3}$$
$$\approx\frac{\eta r_0^3\cos\theta_L}{(a\sin\beta\sin\gamma+h\cos\beta)^3}. \tag{21}$$

With a complex integration as shown in Appendix B, we get the form of the orientational order parameter and the average z-component of the molecular dipole

$$S=\frac{P_z}{P}=\frac{\pi}{Z}\cos\theta_D\sin^2\theta_A+\frac{\pi\eta}{Z}\{\cos\theta_D[(2-3\cos^2\psi)$$
$$\times(\cos^{-1}\theta_A\sin^{-1}\alpha-\sin^{-1}\psi)$$
$$-\sin^2\psi\cos^2\psi(\sin^{-3}\psi-\cos^{-3}\theta_A\sin^{-3}\alpha)]$$
$$+\tan\psi\cos^2\psi\sin\theta_D\cos\phi_D(3\cos^{-1}\theta_A\sin^{-1}\alpha$$
$$-2\sin^{-1}\psi-\sin^2\psi\cos^{-3}\theta_A\sin^{-3}\alpha)\}. \tag{22}$$

It is evident that, besides the partition function Z, the dipole average $\langle P_z\rangle$ apparently separates into two terms: The former is a nonchiral part, whereas the latter includes an apparent chiral factor $\cos\phi_D$. Now it is clear that molecular orientation distribution, and then the statistic property of monolayer, are influenced by the chirality of the component material. The effect of molecular chirality on the MDC behavior of monolayer will be demonstrated in Sec. V.

B. In the case of $|W_s|\ll|W_e|$

In this case, omitting the dipole-image interaction, using Eqs. (4) and (16), the partition function and the orientational order parameter becomes, respectively

$$Z=\int_0^{2\pi}d\gamma\int_0^{\theta_A}\exp(-W_e/kT)\sin\beta d\beta$$
$$=2\pi\int_0^{\theta_A}I_0(\xi S\sin\theta_D\sin\beta)$$
$$\times\exp\{-\xi S\cos\theta_D\cos\beta\}\sin\beta d\beta, \tag{23}$$

and

$$S=\frac{1}{Z}\int_0^{2\pi}\int_0^{\theta_A}\cos\theta_L\exp(-W_e/kT)\sin\beta d\beta d\gamma$$
$$=\frac{2\pi}{Z}\int_0^{\theta_A}\sin\beta d\beta\exp(-\xi S\cos\theta_D\cos\beta)$$
$$\times[\cos\theta_D\cos\beta I_0(\xi S\sin\theta_D\sin\beta)$$
$$-\sin\theta_D\sin\beta I_1(\xi S\sin\theta_D\sin\beta)], \tag{24}$$

where $\xi=gP^2a^{-3/2}/kT$, and

$$I_0(\alpha)=\frac{1}{2\pi}\int_0^{2\pi}\exp[\alpha\sin\gamma]d\gamma,$$
$$I_1(\alpha)=\frac{1}{2\pi}\int_0^{2\pi}\sin\gamma\exp[\alpha\sin\gamma]d\gamma, \tag{25}$$

are the zeroth- and first-order Bessel functions. Two points about Eqs. (23) and (24) should be emphasized. The first is that S and Z involve each other in their equations. This characteristic clearly demonstrates that the present question (the mean-field approach) is a self-consistent one. Secondly, both of these equations do not include ϕ_D, the mark of the molecular chirality. This feature strongly indicates that under the mean-field approach, the molecular chirality has no effect on the electrical properties including the MDC behavior of monolayer. As we mentioned in Sec. III, the mean-field approach may be applicable only if the molecular area A is quite smaller than the critical molecular area A_0. This analysis corresponds well with the experiment result: Although for the chiral and racemic DPPC samples the MDC behavior is different with each other as the molecular area is close to the phase transition area (the anomalous MDC peaks), the MDC curves shown in Fig. 2, at small molecular area, agree well with each other. This agreement intimates that for the present materials the mean-field approach is applicable to the small area case.

Of course the above self-consistent group can be solved through numerical approach, whereas for qualitative demonstration of the mean-field behavior of monolayer dielectric, we simply invoke some series expansion approximation in terms of ξ. This simplification may be viewed as a high-temperature or weak-dipole approximation.

By expanding the Bessel functions into Taylor Series[21] up to the second order (see Appendix C), a calculation leads the partition function and the order parameter to, respectively

$$\frac{Z}{2\pi}=(1-\cos\theta_A)-\frac{1}{2}\xi S\cos\theta_D(1-\cos^2\theta_A)+\frac{1}{12}\xi^2S^2[(2\cos^2\theta_D-\sin^2\theta_D)(1-\cos^3\theta_A)+3\sin^2\theta_D(1-\cos\theta_A)] \tag{26}$$

and

$$\frac{ZS}{2\pi}=\frac{1}{2}\cos\theta_D(1-\cos^2\theta_A)+\frac{1}{6}\xi S[-2\cos^2\theta_D(1-\cos^3\theta_A)-3\sin^2\theta_D(1-\cos\theta_A)+\sin^2\theta_D(1-\cos^3\theta_A)]+\frac{1}{16}\xi^2S^2[(1-\cos^4\theta_A)(2\cos^3\theta_D-3\cos\theta_D\sin^2\theta_D)+6\cos\theta_D\sin^2\theta_D(1-\cos^2\theta_A)]. \tag{27}$$

The combination of Eqs. (26) and (27) leads us to an equation about S without involvement with the partition Z

$$S=\left[\frac{ZS}{2\pi}\right]\times\left[\frac{Z}{2\pi}\right]^{-1}=\frac{1}{2}\cos\theta_D(1+\cos\theta_A)+\frac{1}{12}\xi S[(-4+2\cos\theta_A+2\cos^2\theta_A)+3\cos^2\theta_D\sin^2\theta_A]-\frac{1}{16}\xi^2S^2\cos\theta_D\sin^2\theta_D\times\sin^2\theta_A(1-\cos\theta_A). \tag{28}$$

This is an equation about S with the form $S=\lambda_0+\lambda_1\xi S+\lambda_2\xi^2S^2$. An iteration program leads to $S=\lambda_0[1+\lambda_1\xi+(\lambda_1^2+\lambda_0\lambda_2)\xi^2]$. At last we get

$$S=\frac{1}{2}\cos\theta_D(1+\cos\theta_A)\left\{1+\frac{1}{12}\xi[(-4+2\cos\theta_A+2\cos^2\theta_A)+3\sin^2\theta_A\cos^2\theta_D]+\frac{1}{288}\xi^2[2(-4+2\cos\theta_A+2\cos^2\theta_A)^2+12\cos^2\theta_D\sin^2\theta_A(-4+2\cos\theta_A+2\cos^2\theta_A)+18\cos^4\theta_A-9\sin^2\theta_D\cos^2\theta_D\sin^4\theta_A]\right\}. \tag{29}$$

It is easy to check that, as the interaction parameter ξ is set to be zero, the orientational order parameter returns to S_0, which is the orientational order parameter as the interaction on molecules is negligible. Noting that the first order coefficient of ξ

$$\tfrac{1}{12}[(-4+2\cos\theta_A+2\cos^2\theta_A)+3\sin^2\theta_A\cos^2\theta_D],$$

is positive definite, we can conclude that the orientational order parameter with mean-field interaction is smaller than that of no interaction, i.e., the orientational order is suppressed due to the repulsive interaction working between molecules. This result is well consistent with the fact that juxtaposed dipoles with parallel orientation always repulse each other. This repulsion may be one origin of the 2D interfacial pressure, at least in the case of small molecular area. In Fig. 5 we show a S diagram calculated based on mean-field approach, with ξ as parameter. From this figure it is clearly seen that the profile of $S-A$ curve is modified by the relative interaction strength ξ.

V. CALCULATION AND DISCUSSION

In order to clarify the feature of $\langle P_z\rangle$, we plot the orientational order parameter S as a function of A/A_0 $(=\sqrt{1-\cos^2\theta_A})$, with η, ψ, θ_D, and ϕ as parameters under

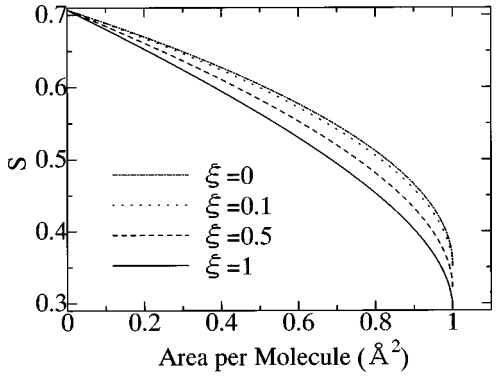

FIG. 5. Mean-field behavior of the orientational order parameter ($\theta_D = \pi/4$).

the assumption $|W_s| \gg |W_e|$. In Fig. 6 we plot some examples of our calculation based on Eq. (22). As DPPC molecule is rather complex, it is difficult to find the proper correspondence between the real molecule and our present model. So for simplicity, as a representative example, in Fig. 6 we only show some curves with $\eta = 0.02$, which is a typical quantity for amphiphiles at room temperature, and $\psi = \pi/4$, which means that the model parameters $h = a$. Figures 6(a) and 6(b) include some order parameter curves with different θ_D and ϕ_D. It is clearly seen that the order parameter S behaves rather differently at large molecular area region for various chiral angle ϕ_D. The difference is enlarged as θ_D increases, and reaches the maximum as $\theta_D = \pi/2$. For some cases, such as curve 4 in Fig. 6(b), the order parameter increases from a positive value at $A/A_0 = 0$ to a larger positive one at $A/A_0 = 0.5$. These phenomena evidently, though much roughly, demonstrate the effect of the molecular chirality on the polar properties of amphiphile monolayers.

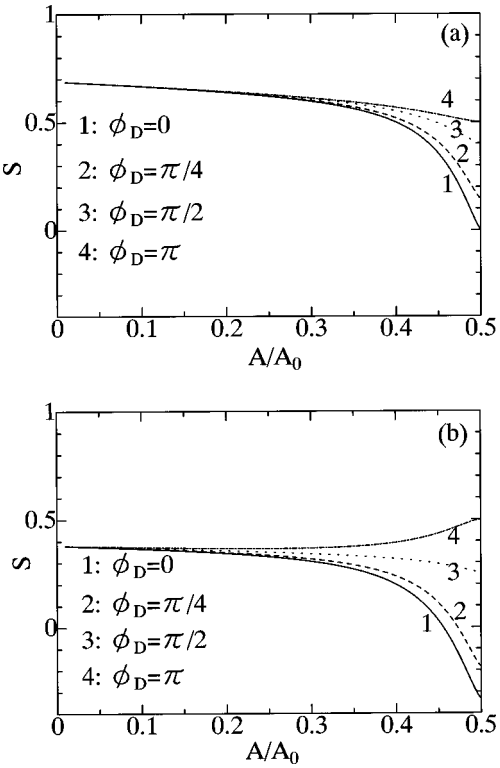

FIG. 6. Orientational order parameter S as a function of the molecular area A/A_0 for various θ_D and ϕ_D. (a) $\eta = 0.02$, $\theta_D = \pi/4$, and $\psi = \pi/4$, (b) $\eta = 0.02$, $\theta_D = 3\pi/8$, and $\psi = \pi/4$.

The curves with different ϕ_D but same θ_D meet each other at $A = 0$, $S = \cos\theta_D$. It means that at the limit of $A = 0$, all the molecular axis parallel to each other and normal to the monolayer plane. Noting that at the limit $A = 0$, the molecular dipoles are not normal to the monolayer plane but with a cross-angle θ_D, it is easy to know that at this limit the order parameter S, which represents the average direction of dipoles, reaches $\cos\theta_D$, not 1.

S in the range of $0.5 < A/A_0 < 1$ is not calculated, because as $A > 0.5$, for the present molecular angle $\psi = \pi/4$, it is possible that the dipole submerges into the water surface. This leads to a divergence of calculation and the meaning of the order parameter is obscure.

We also studied the MDC behavior of monolayer with this model. As described in the previous paper,[11] the MDC generated by monolayer compression is calculated from the following equation:

$$I = \frac{B\gamma_0}{dA}\left(\frac{\langle P_z\rangle}{A} - \frac{d\langle P_z\rangle}{dA}\right), \tag{30}$$

where B is the working area of the electrode, γ_0 is the compression speed of the monolayer and d is the spacing between the top electrode and the water surface. We computed $I' [= I/(B\gamma_0/d)]$ as a function of A using Eq. (22), with the same parameters as shown in Fig. 6. The result of computation is shown in Fig. 7. As seen in Figs. 7(a) and 7(b), for different chiral angle ϕ_D, the MDC behavior is much different in the region of $0.4 < A < 0.5$. Positive and negative peaks are both available as well as flat plateau. All these configurations strongly demonstrate the chirality of constituent molecules as an important factor of the electrical properties, especially the MDC behavior. For small area region all the MDC curves are convergent with a $1/A^2$ style of manner.

As has been discussed previously, the MDC in $0.5 < A/A_0 < 1$ region is not calculated because of divergence. In our experiments, the MDC curves on the right side of the anomalous peaks are with strange behavior and little reappearance. The cause of this eccentricity is still unknown.

The behaviors of MDC for different η and ψ are also investigated. We found that η mainly affects the height of the MDC peaks, whereas with little action on the profile of the curves. The value of ψ determines the right edge of the MDC graphs [for $\psi = \pi/4$, $(A/A_0)_{\max} = 0.5$] and slightly affects the MDC peak profile (flat or sharp). Both η and ψ do not change the direction (up or down) of the peaks (not shown here).

We can compare the theoretical MDC curve with the experimental one. The racemic DL-DPPC molecule corresponds to the theoretically achiral cases of $\phi_D = 0$ or π. The

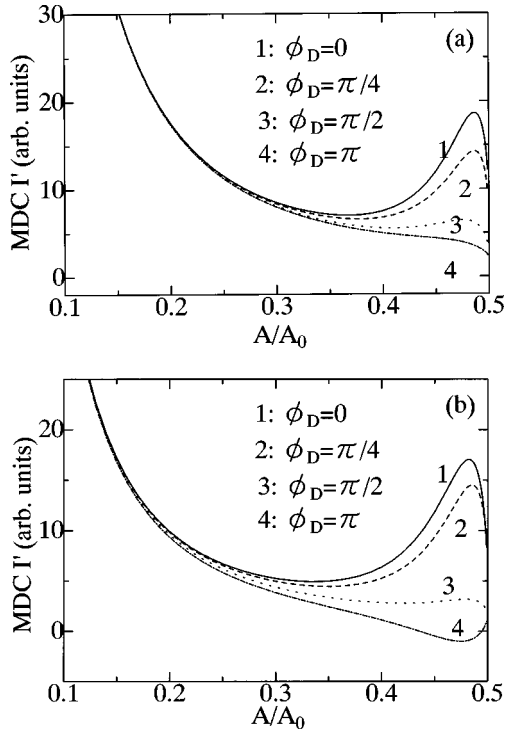

FIG. 7. MDC flowing across a monolayer composed of chiral molecules on the air–water interface by monolayer compression for various θ_D and ϕ_D. (a) $\eta=0.02$, $\theta_D=\pi/4$, and $\psi=\pi/4$, (b) $\eta=0.02$, $\theta_D=3\pi/8$, and $\psi=\pi/4$.

chiral angles of D- and L-DPPC molecules should have identical absolute value but contrary sign. In Fig. 7 we can see that, the anomalous peak of DL-DPPC is upward, which implies that it is the case of $\phi_D=0$. The reason is still unknown why the behavior of the DL-DPPC monolayer is similar to the theoretical case of $\phi_D=0$ but not $\phi_D=\pi$. For the chiral cases of D- and L-DPPC, the theory predict that their MDC behavior is the same (the sign of the chiral angle ϕ_D has no effect on the MDC behavior of monolayers). This is approved by the experiment: Although as $A>90\,\text{Å}^2$ (corresponding to the LE phase), the MDC curves is a little unstable and the reappearance is not so good, in the $65\,\text{Å}^2 < A < 85\,\text{Å}^2$ region (the flat plateau of the $\pi-A$ isotherm, or the 2D phase transition region), the compression of D- and L-DPPC monolayer always generate downward peaks similar well to each other, which strongly contrast with the upward peak of DL-DPPC.

As a tentative work we established this simple model to describe the molecular chirality of monolayer and try to use this model to explain some experimental results of MDC measurement. By using this model, we show the electrical properties, especially the MDC behavior, depend on the chirality of the molecules. The experiment also demonstrates this point. Nevertheless, although the model qualitatively shows that the MDC of monolayer is chirality-related, the agreement between the experiment and the theory is still phenomenological. The two achiral cases ($\phi_D=0$ and π) have quite different theoretical behaviors, whereas we cannot still clearly understand why the DL-DPPC behaves similar to one of them ($\phi_D=0$) but not the other ($\phi_D=\pi$). Further, the chiral angle of the DPPC molecules satisfying the experimental MDC curve is not easy to be determined. For these reasons, this model is to be improved in the future work. We also did some experiment of MDC measurement about mixing of D- and L-DPPC monolayers with different ratios. The results are partly shown in our previous work[13] but not here. The results of mixing monolayers also accommodate some important messages about molecular chirality and monolayer organization properties. To analyze the mixing monolayer, it is necessary to consider intermolecular actions. These will be done in our future work.

VI. CONCLUSION

For centuries scientists have been researching the relationship between microscopic structure and macroscopic properties of materials. We also devoted to this motif. We demonstrated the molecular chiral effect on macroscopic electrical properties of monolayers, both experimentally and theoretically. We found that for different samples of DPPC the MDC behavior is divergent, with the anomalous peaks as the most dominant characteristic. We detailedly analyzed the chiral molecular model constructed in our previous paper.[13] The calculation showed that for different parameters (especially different chiral angle ϕ_D), the model give distinct MDC behaviors, which partly agree with the experiment. The mean-field approach showed that in small area region, the chirality has no effect on MDC behavior. This point corresponds well with the experiment. Briefly, in the theoretical aspect, the present work indicate that this molecular model, though conceptually simple, is useful in the investigation of chirality; on the experimental side, our work shows that MDC technique may be rather useful in the researching of molecular chirality and related topics, such as chiral discrimination and chiral phase separation.

APPENDIX A

Considering the following formulas:

$$\int_0^{2\pi}\frac{d\gamma}{a\sin\beta\sin\gamma+h\cos\beta}=\frac{2\pi}{\sqrt{h^2\cos^2\beta-a^2\sin^2\beta}},$$

$$\int_0^{2\pi}\frac{d\gamma}{(a\sin\beta\sin\gamma+h\cos\beta)^2}=\frac{2\pi h\cos\beta}{(h^2\cos^2\beta-a^2\sin^2\beta)^{3/2}},$$

$$\int_0^{2\pi}\frac{d\gamma}{(a\sin\beta\sin\gamma+h\cos\beta)^3}=\frac{\pi(a^2\sin^2\beta+2h^2\cos^2\beta)}{(h^2\cos^2\beta-a^2\sin^2\beta)^{5/2}}, \tag{A1}$$

the integration with respect to γ in Eq. (18) can be carried out

$$\int_0^{2\pi}\Omega d\gamma=\pi\frac{(a^2\sin^2\beta+2h^2\cos^2\beta)}{(h^2\cos^2\beta-a^2\sin^2\beta)^{5/2}}+\pi\cos^2\theta_D\frac{(a^2\sin^2\beta\cos^2\beta+2h^2\cos^4\beta)}{(h^2\cos^2\beta-a^2\sin^2\beta)^{5/2}}+\pi\sin^2\theta_D\cos^2\phi_D$$
$$\times\frac{2a^2\sin^4\beta+h^2\sin^2\beta\cos^2\beta}{(h^2\cos^2\beta-a^2\sin^2\beta)^{5/2}}+\pi\sin^2\theta_D\sin^2\phi_D\frac{h^2\sin^2\beta\cos^2\beta-a^2\sin^4\beta}{(h^2\cos^2\beta-a^2\sin^2\beta)^{5/2}}-3\pi ah\sin 2\theta_D$$
$$\times\cos\phi_D\frac{\sin^2\beta\cos^2\beta}{(h^2\cos^2\beta-a^2\sin^2\beta)^{5/2}},\tag{A2}$$

Eq. (A2) is integrated with respect to $\sin\beta d\beta$ term by term

$$\int_0^{\theta_A}\frac{a^2\sin^2\beta+2h^2\cos^2\beta}{(h^2\cos^2\beta-a^2\sin^2\beta)^{5/2}}\sin\beta d\beta=\frac{2-3\cos^2\psi}{r_0^3}B_2+\frac{\cos^2\psi}{r_0^3}B_0,$$

$$\int_0^{\theta_A}\frac{a^2\sin^2\beta\cos^2\beta+2h^2\cos^4\beta}{(h^2\cos^2\beta-a^2\sin^2\beta)^{5/2}}\sin\beta d\beta=\frac{2-3\cos^2\psi}{r_0^3}B_4+\frac{\cos^2\psi}{r_0^3}B_2,$$

$$\int_0^{\theta_A}\frac{2a^2\sin^4\beta+h^2\sin^2\beta\cos^2\beta}{(h^2\cos^2\beta-a^2\sin^2\beta)^{5/2}}\sin\beta d\beta=\frac{2-3\sin^2\psi}{r_0^3}B_4+\frac{1-5\cos^2\psi}{r_0^3}B_2+\frac{2\cos^2\psi}{r_0^3}B_0,$$

$$\int_0^{\theta_A}\frac{h^2\sin^2\beta\cos^2\beta-a^2\sin^4\beta}{(h^2\cos^2\beta-a^2\sin^2\beta)^{5/2}}\sin\beta d\beta=-\frac{1}{r_0^3}B_4+\frac{1+\cos^2\psi}{r_0^3}B_2-\frac{\cos^2\psi}{r_0^3}B_0,$$

$$\int_0^{\theta_A}\frac{ah\sin^2\beta\cos^2\beta}{(h^2\cos^2\beta-a^2\sin^2\beta)^{5/2}}\sin\beta d\beta=-\frac{\sin\psi\cos\psi}{r_0^3}B_4+\frac{\sin\psi\cos\psi}{r_0^3}B_2,\tag{A3}$$

where

$$B_0=\int_{\cos\theta_A}^1\frac{dx}{(x^2-\cos^2\psi)^{5/2}}=\frac{1}{\cos^4\psi}\left[\left(\frac{1}{\sin\psi}-\frac{1}{\sin\alpha}\right)-\frac{1}{3}\left(\frac{1}{\sin^3\psi}-\frac{1}{\sin^3\alpha}\right)\right],$$

$$B_2=\int_{\cos\theta_A}^1\frac{x^2}{(x^2-\cos^2\psi)^{5/2}}dx=-\frac{1}{3\cos^2\psi}\left(\frac{1}{\sin^3\psi}-\frac{1}{\sin^3\alpha}\right),$$

$$B_4=\int_{\cos\theta_A}^1\frac{x^4}{(x^2-\cos^2\psi)^{5/2}}dx=-\frac{1}{\sin\psi}+\frac{1}{\sin\alpha}-\frac{1}{3\sin^3\psi}+\frac{1}{3\sin^3\alpha}+\ln\left|\frac{1+\sin\psi}{\cos\theta_A(1+\sin\alpha)}\right|.\tag{A4}$$

The substitution of Eqs. (A2)–(A4) at last leads Eq. (18) to Eq. (19).

APPENDIX B

The integration in terms of γ in the second term of Eq. (20) is performed as

$$\int_0^{2\pi}d\gamma\frac{\cos\theta_L}{(a\sin\beta\sin\gamma+h\cos\beta)^3}d\gamma=\pi\cos\theta_D\frac{(a^2\sin^2\beta+2h^2\cos^2\beta)\cos\beta}{(h^2\cos^2\beta-a^2\sin^2\beta)^{5/2}}$$
$$+2\pi\sin\theta_D\cos\phi_D\frac{h\cos\beta}{a(h^2\cos^2\beta-a^2\sin^2\beta)^{3/2}}-\pi\sin\theta_D\cos\phi_D\frac{h\cos\beta(2h^2\cos^2\beta+a^2\sin^2\beta)}{a(h^2\cos^2\beta-a^2\sin^2\beta)^{5/2}}.\tag{B1}$$

The integrals with respect to β are dealt with as follows term by term:

$$\int_0^{\theta_A}\frac{(a^2\sin^2\beta+2h^2\cos^2\beta)\cos\beta}{(h^2\cos^2\beta-a^2\sin^2\beta)^{5/2}}\sin\beta d\beta=\frac{2-3\cos^2\psi}{r_0^3}F_1+\frac{\cos^2\psi}{r_0^3}F_2,$$

$$\int_0^{\theta_A}\frac{h\cos\beta}{a(h^2\cos^2\beta-a^2\sin^2\beta)^{3/2}}\sin\beta d\beta=\frac{\tan\psi}{r_0^3}F_3,$$

$$\int_0^{\theta_A}\frac{h}{a}\frac{(2h^2-a^2)\cos^3\beta+a^2\cos\beta}{(h^2\cos^2\beta-a^2\sin^2\beta)^{5/2}}\sin\beta d\beta=\frac{\tan\psi}{r_0^3}[(2-3\cos^2\psi)F_1+\cos^2\psi F_2],\tag{B2}$$

where

$$F_1=\int_{\cos\theta_A}^{1}\frac{x^3}{(x^2-\cos^2\psi)^{5/2}}dx$$
$$=(\cos^{-1}\theta_A\sin^{-1}\alpha-\sin^{-1}\psi)$$
$$-\tfrac{1}{3}\cos^2\psi(\sin^{-3}\psi-\cos^{-3}\theta_A\sin^{-3}\alpha),$$
$$F_2=\int_{\cos\theta_A}^{1}\frac{x}{(x^2-\cos^2\psi)^{5/2}}dx$$
$$=-\tfrac{1}{3}(\sin^{-3}\psi-\cos^{-3}\theta_A\sin^{-3}\alpha),$$
$$F_3=\int_{\cos\theta_A}^{1}\frac{x}{(x^2-\cos^2\psi)^{3/2}}dx$$
$$=\cos^{-1}\theta_A\sin^{-1}\alpha-\sin^{-1}\psi. \quad \text{(B3)}$$

Inserting them into Eq. (20), we get, finally, Eq. (22).

APPENDIX C

At first, we expand the Bessel functions into Taylor series[21]

$$I_0(\alpha)=\sum_{k=0}^{\infty}\frac{(\alpha/2)^{2k}}{(k!)^2}=1+\frac{\alpha^2}{4}+\frac{\alpha^4}{64}\cdots,$$
$$I_1(\alpha)=\sum_{k=0}^{\infty}\frac{(\alpha/2)^{2k+1}}{k!(k+1)!}=\frac{\alpha}{2}+\frac{\alpha^3}{16}\cdots. \quad \text{(C1)}$$

Up to the second order of ξ, the partition and order parameter becomes, respectively

$$Z=2\pi[1+\tfrac{1}{4}\xi^2S^2\sin^2\theta_D]\cdot J_0-2\pi\tfrac{1}{4}\xi^2S^2\sin^2\theta_D\cdot J_2,$$
$$S=\frac{2\pi}{Z}\Big[\cos\theta_D(1+\tfrac{1}{4}\xi^2S^2\sin^2\theta_D)\cdot J_1-\tfrac{1}{4}\xi^2S^2\cos\theta_D$$
$$\times\sin^2\theta_D\cdot J_3-\tfrac{1}{2}\xi S\sin^2\theta_D\cdot J_0+\tfrac{1}{2}\xi S\sin^2\theta_D\cdot J_2, \quad \text{(C2)}$$

where the integrals J_i, $i=0$, 1, 2, and 3, as well as their expansion, are

$$J_0=\int_{\cos\theta_A}^{1}\exp(-\mu x)dx$$
$$=(1-\cos\theta_A)-\tfrac{1}{2}\mu(1-\cos^2\theta_A)+\tfrac{1}{6}\mu^2(1-\cos^2\theta_A), \quad \text{(C3)}$$
$$J_1=\int_{\cos\theta_A}^{1}x\exp(-\mu x)dx$$
$$=\tfrac{1}{2}(1-\cos^2\theta_A)-\tfrac{1}{3}\mu(1-\cos^3\theta_A)+\tfrac{1}{8}\mu^2(1-\cos^4\theta_A),$$
$$J_2=\int_{\cos\theta_A}^{1}x^2\exp(-\mu x)dx$$
$$=\tfrac{1}{3}(1-\cos^3\theta_A)-\tfrac{1}{4}\mu(1-\cos^4\theta_A)+\tfrac{1}{10}\mu^2(1-\cos^5\theta_A),$$
$$J_3=\int_{\cos\theta_A}^{1}x^3\exp(-\mu x)dx$$
$$=\tfrac{1}{4}(1-\cos^4\theta_A)-\tfrac{1}{5}\mu(1-\cos^5\theta_A)+\tfrac{1}{12}\mu^2(1-\cos^6\theta_A).$$

An insertion of Eq. (C3) into Eq. (C2) leads just to Eqs. (26) and (27).

[1] M. N. Jones and D. Chapman, *Micelles, Monolayers and Biomembranes* (Wiley, New York, 1995), p. 24.
[2] W. M. Gelbart, A. Ben-Shaul, and D. Roux, *Micelles, Membranes, Microemulsions and Monolayers* (Springer-Verlag, New York, 1994), Chap. 12.
[3] I. Langmuir, J. Chem. Phys. **1**, 756 (1933).
[4] K. Blodgett, J. Am. Chem. Soc. **56**, 1007 (1935).
[5] M. Iwamoto, Y. Majima, H. Naruse, T. Noguchi, and H. Fuwa, Nature (London) **353**, 645 (1991).
[6] A. Collet, M. J. Brienne, and J. Jacques, Chem. Rev. **80**, 215 (1980).
[7] C. J. Eckhardt, N. M. Peachey, D. R. Swanson, J. M. Takacs, M. A. Khan, X. Gong, J. H. Kim, J. Wang, and U. A. Uphans, Nature (London) **362**, 614 (1993).
[8] For a review, see S. Mason, Chem. Soc. Rev. **17**, 347 (1988).
[9] L. Pasteur, Ann. Phys. (Leipzig) **24**, 442 (1848).
[10] N. Nandi and B. Bagchi, J. Am. Chem. Soc. **118**, 11208 (1996).
[11] A. Sugimura, M. Iwamoto, and Z. C. Ou-Yang, Phys. Rev. E **50**, 614 (1994); **54**, 6537 (1996); Chem. Phys. Lett. **274**, 505 (1997).
[12] C. X. Wu, Z. C. Ou-Yang, and M. Iwamoto, J. Chem. Phys. **109**, 4552 (1998).
[13] Z. C. Ou-Yang, X. B. Xu, C. X. Wu, and M. Iwamoto, Phys. Rev. E **59**, 2105 (1999).
[14] M. Iwamoto, T. Kubota, and Z. C. Ou-Yang, J. Chem. Phys. **104**, 736 (1996).
[15] T. Tachibana, T. Yoshizumi, and K. Hori, Bull. Chem. Soc. Jpn. **52**, 34 (1979).
[16] P. G. de Gennes, *The Physics of Liquid Crystals* (Clarendon, Oxford, 1966).
[17] M. E. Rose, *Elementary Theory of Angular Momentum* (Wiley, New York, 1957).
[18] N. Israelachvili, *Intermolecular and Surface Forces* (Academic, London, 1992), p. 28.
[19] M. Iwamoto, Y. Mizutani, and A. Sugimura, Phys. Rev. B **54**, 8186 (1996).
[20] L. Onsager, Ann. (N.Y.) Acad. Sci. **51**, 627 (1949).
[21] I. S. Gradshteyn and I. M. Ryzhik, *Table of Integrals, Series, and Products* (Academic, Orlando, 1980).